Hyperfine Interact (2016) 237:8
DOI 10.1007/s10751-016-1221-9

The hyperfine properties of iron-gallium alloys

M. Elzain[1] · A. Gismelseed[1] · A. Al-Rawas[1] · A. Yousif[1] · H. Widatallah[1] · Maya Al-Azri[1] · M. Al-Barwani[2]

Abstract The hyperfine properties at Fe site in iron-gallium alloy are calculated using the full-potential linear-augmented-plane-waves method. We have calculated the Fermi contact field (B_{hf}) and isomer shift (δ) at the Fe site versus the number of neighbouring Ga atoms. We found that B_{hf} decrease whereas δ increases with increasing number of neighbouring G atom. In addition we have calculated the hyperfine properties of FeGa system with DO_3 structure, where various distributions of 4 the Ga atoms in the conventional unit cell are considered (including the regular DO_3 structure). We found that the DO_3 structure has the lowest energy as compared to the other configurations. The two distinct A and D sites of the ordered DO_3 conventional unit cell have two distinct values for B_{hf} and δ. On changing the atomic arrangement of the Ga atoms within the conventional unit cell, the configuration of the A site is maintained whereas that of the D site becomes imperfect. The contact magnetic hyperfine fields of the D-like sites in the imperfect structures are lower than that of the DO_3D site.

Keywords Isomer shift · Hyperfine field · Phases

1 Introduction

The iron-gallium alloys possess large magnetostriction that promises potential applications as sensors and actuators [1]. The Fe-Ga alloys supersede other materials through their low

This article is part of the Topical Collection on *Proceedings of the International Conference on the Applications of the Mössbauer Effect (ICAME 2015), Hamburg, Germany, 13–18 September 2015*

✉ M. Elzain
elzain@squ.edu.om

[1] Department of Physics, Sultan Qaboos University, Box 36, Al Khod 123, Oman

[2] NYU Abu Dhabi, Box 129188, Abu Dhabi, United Arab Emirates

Published online: 18 February 2016

cost, good ductility, weak magnetostriction coefficient temperature dependence and low saturation fields.

The magnetostriction of Fe-Ga alloys depends on Ga concentration. It exhibits double peaks at about 19 and 28 at % Ga concentration with a minimum at about 23 % Ga [2]. Its maximum value exceeds that of pure α-Fe by an order of magnitude. The value of the magnetostriction of Fe-Ga alloys depends on their thermal history. Higher values are obtained for quenched alloys, while slow cooled and annealed samples show lower magnetostriction.

The increase in magnetostriction for Ga concentration less than 19 %, is attributed to reduction in magnetocrystalline anisotropy since it was observed that the two quantities show opposite trends with increasing Ga concentration [3]. In this range Fe-Ga alloys retain the disordered bcc A2 phase. Around 19 % Ga the bcc ordered DO_3 appears. In one approach to the explanation of the magnetostriction curve, the appearance of the DO_3 phase in combination with the A2 phase is assumed to be detrimental to magnetostriction and it is behind the decrease of its value beyond 19 % Ga [4]. The decrease of magnetostriction continues in the presence of the mixed phase up to around 23 % Ga. Beyond this concentration, the DO_3 phase dominates and the magnetostriction increases again. The second peak in the magnetostriction at around 28 % Ga is assumed to result from the softening of the tetragonal shear modulus of the DO_3 phase [5]. The appearance of other precipitates for concentrations more than about 28 % of Ga results in decreasing the magnetostriction.

A number of phases like the bcc B2 and fcc DO_{22} were also considered to be present in Fe-Ga alloys in different concentration ranges [6–10]. In an alternative approach, the origin of magnetostriction is attributed to the rotation of heterogeneous tetragonal precipitates like DO_{22} in the matrix of A2 phase on application of external field [11]. A number of recent publications report the presence of some precipitates [12–14], while the absence of such precipitates is also reported [15].

The average lattice constant was found to increase linearly with Ga content whereas, the magnetization and the average hyperfine field decrease linearly [10, 16]. Newkirk and Tsuei [17] measured the hyperfine field and isomer shift of quenched Fe-Ga alloys and determined an empirical formula that relates the magnetic hyperfine field to the number of nearest and next nearest neighboring Ga atoms for Ga concentrations up to 25 %. Dunlap et. al. [18] found no evidence of DO_3 phase for Ga concentrations up to 20.5 % in rapidly quenched samples. For the sample with 23.3 % Ga concentration, their Mossbauer measurement indicated the presence of DO_3 and the fcc $L1_2$ phases. The isomer shift was found to increase with Ga concentration and values of +0.28, 0.11 and 0.22 mm/s were reported for DO_3 (A and D-sites) and $L1_2$ respectively. Mellors et. al. [16] carried a detailed study using both Mossbauer spectroscopy and high resolution neutron diffraction of both as-quenched and annealed samples with Ga contents up to 22.5 %. For concentrations less than 22.5 % the bcc A2 is retained in all samples, while for the 22.5 % the DO_3 phase was detected but no signals for $L1_2$ phase were found. The presence of a tetragonally distorted DO_3 phase is indicated instead of the $L1_2$ phase. Basumatary et. al. [19] reported minor fraction of DO_3 and $L1_2$ phases for concentrations greater than 25%. Blachowski et. al [20] studied the bcc disordered alloys up to 29 % Ga concentration and found that the major contribution to the reduction of the magnetic hyperfine results from the Ga nearest neighbors of Fe. On the other hand they found that a Ga atom at next nearest neighbor site contributes to the increase in the isomer shift about double that of Ga atom at the nearest neighbors. Blachowski and Wdowik [21] used the full-potential linearized augmented plane abinitio method to calculate the perturbation in charge and spin densities at Fe sites due to different impurities including Ga. Their results were found to correlate well to experimental data.

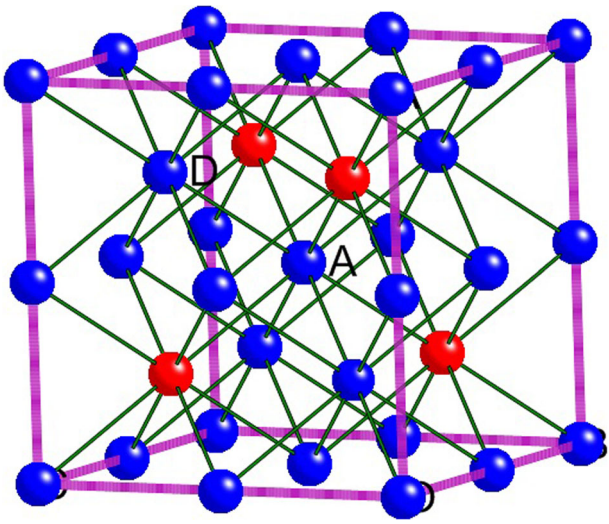

Fig. 1 The $2 \times 2 \times 2$ supercell used to calculate the electronic structure of Fe-Ga alloys. The figure shows the supercell corresponding to DO_3 where blue balls represent Fe and red balls are Ga. The supercell consists of 8 conventional BCC unit cells. 4 of the 8 atoms at the body center of the conventional unit cell are Ga atoms. The remaining 4 are Fe D sites of zero Ga neighbors (see label). The atoms at the corners of the conventional BCC unit cell form Fe A sites of 4 Ga neighbors (see label). For other configurations the number of atoms and atomic positions are changed according to the structure under study

Wang et. al. [22] used density functional theory together with molecular dynamics simulation and demonstrated that the formation of DO_3 structure leads to the softness of the tetragonal shear modulus. In addition Wang et. al. [23] studied B2 and DO_3 clusters in A2 phase and concluded that nanoprecipitates cannot be the reason behind the large Fe-Ga magnetostriction. On the other hand, Boisse et. al. [24] used modelling and atomic field approximation and concluded that phase transformation of A2 into tetragonally distorted DO_3 and $L1_0$ precipitates goes through transient B2 structures and they attributed the origin of magnetostriction to these precipitates.

In the following section we outline our computational method, then we present and discuss the results of our calculation of the magnetic and hyperfine properties of Fe-Ga alloys in Section 3. A short conclusion is presented in the last section. Our objective is to consider the hyperfine properties of different phases and to identify features that can easily be used to distinguish between phases.

2 Computational Method

To study the effect of introducing Ga atoms into Fe on its hyperfine properties, we used supercells composed of $2 \times 2 \times 2$ conventional bcc unit cells. The lattice constant corresponding to each structure is obtained through volume optimization. Figure 1 shows the supercell structure corresponding to DO_3.

The full-potential linear-augmented-plane –wave (FP-LAPW) method as employed in the WIEN2k package.) [25] is used to calculate the electronic and magnetic properties of Fe-Ga alloys.

Table 1 The local magnetic moment, m, in Bohr Magnetrons, the Fermi contact hyperfine field, B_{hf} in Teslas, the isomer shift and δ (relative to α-Fe) in mm/s at Fe sites versus the number of neighboring Ga atoms (N)

N	1	2	3	4
m (μ_B)	2.26	2.33	2.22	2.08
B_{hf}(T)	29.5	29.0	27.0	26.0
δ (mm/s)	0.01	0.08	0.14	0.18

In the L/APW+lo method the Kohn-Sham orbitals are expanded in terms of atomic orbitals inside the atomic muffin-tin (MT) sphere of radius R_{MT} and in terms of plane waves in the interstitial regions. The Kohn-Sham equations were solved using Perdew-Burke-Ernerhof GGA approximation. Core and valence states were separated by an atomic energy of -6.0 Ry. For the valence electrons the potential and charge density are expanded in spherical harmonics up to L = 4, while the wavefunctions are expanded inside the MT sphere up to $l = 10$ partial waves. Mixed basis are used depending on the partial wave l with APW+lo being used for s, p and d valence orbitals. LAPW is used for the remaining l values. For the plane wave expansion in the interstitial region we have used wavenumber cut off K_{max} such that $R_{MT} K_{max} = 7.0$ and the potential and charge density are Fourier expanded with $G_{\max} = 14.0$. The mesh size and the number of points in the Brillouin zone were tested for the conventional unit cell using the convergence of the values of the electric field gradient and the total energy as indicators. A k -sampling with a $6 \times 6 \times 6$ Monkhost-Pack mesh and 108 k –points in the reduced Brillouin zone are used in each supercell.

3 Results and discussion

Using the supercells as in Fig. 1 we have calculated the properties of α-Fe and obtained 31.2 T for the magnitude of the contact magnetic hyperfine field at Fe site and 6.98 a.u. for the valence contact charge density.

In Table 1 we show the local magnetic moment m, the contact magnetic hyperfine field $B_{hf}$and the isomer shift δ at Fe sites (relative to α-Fe) with one, two, three and four Ga atoms at the nearest neighbor sites. It is seen that the magnetic hyperfine field decreases, while the isomer shift increases with increasing number of Ga atoms.

The decrease in the local magnetic moment at Fe site is due to the increase in the $sp-d$ mixing. The reduction in the contact hyperfine field is attributed to the reduction in its core contribution component that is proportional to the local magnetic moment. The increase in the isomer shift is attributed to the decrease of the weight of the s electrons at the Fe site resulting from the $sp-d$ mixing. We found that at the same lattice constant the valence contact charge density at the Fe site decreases with increasing Ga atoms at the neighboring sites.

Comparison of B_{hf} to experimental trends of Newkirk and Tsuei [17] is shown in Fig. 2. In this figure the magnetic hyperfine fields are scaled by the corresponding field ofα-Fe. Similar experimental trends were reported in [26]. This will mask the difference in values of the experimental and theoretical results and is expected to exhibit the trends with changing number of nearest neighbors. Note that the generally small and positive in sign orbital and dipolar contributions to magnetic hyperfine field are not included here. Their inclusion may reduce the total theoretical values.

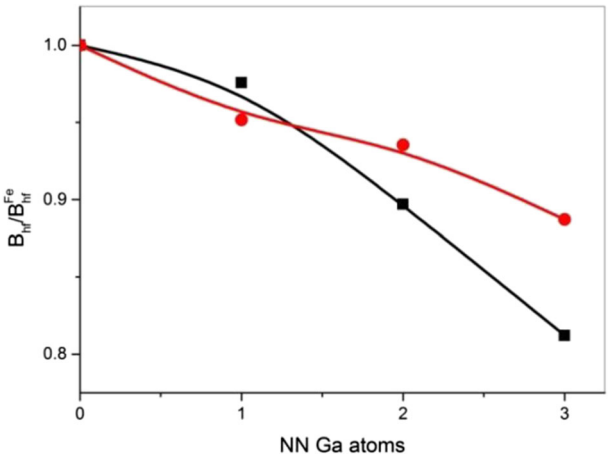

Fig. 2 The scaled experimental ([17]) (black square) and theoretical (red disc) hyperfine field at Fe site versus the number of nearest neighboring Ga atoms. The hyperfine fields are scaled by the corresponding α-Fe fields to exhibit the trends of changing the number of nearest neighbors

In addition to the DO_3 structure exhibited in Fig. 1, we considered different distributions where the 4 Ga atoms are located around the Fe atom in the center of the supercell. Our purpose is to find out the hyperfine properties resulting from a random distribution of the 4 Ga atoms as compared to those of the regular DO_3 structure (denoted in Table 2 by S1). The four Ga atoms are located at the nearest sites surrounding the central Fe atom. In the configuration S2, the Ga atoms are placed directly above each other rather than being rotated at right angle as in DO_3 structure. This corresponds to Ga-Ga pairs which are expected to be behind the large magnetostriction. In S3 the four Ga atoms are placed on one face of the inner cube, while for S4 structure one of S3 Ga atoms is placed at the opposite face. Among the 4 structures studied the S1 structure takes the lowest energy. Results for the 4 different distributions are shown in Table 2. Two distinct Fe sites are obtained for three of the distribution and the fourth leads to four distinct Fe sites within the supercell. The first row for each property corresponds to the Fe A site with 4 neighboring Ga atoms and none at second and third neighboring sites. For S4 the first values in the first row of the combination correspond to the A site. The second values in the first row and those in the second row corresponds to the Fe D sites and its imperfect versions resulting from changing of position of the Ga atoms. The imperfect D sites differ in the number of Ga atoms at the second and third neighboring sites of the Fe atom as compared to DO_3. In general the A sites possess low magnetic hyperfine field and high isomer shift, while the D like sites have high hyperfine field and low isomer shift. In general, the calculated contact hyperfine fields are larger than the corresponding reported experimental results [16, 18]

We note that both the isomer shifts and the contact hyperfine fields do not vary that much between the different equivalent sites. The imperfect structures, in addition to the regular DO_3 may be observed in a quenched sample leading to a distribution of magnetic hyperfine fields.

The results of the calculations on systems with B2 structure give a small magnetic hyperfine field of order of 13 T and a high isomer shift of order 0.40 mm/s. Borrego et. al. [26] and Javed et. al. [27] reported such low fields in their quenched alloys and thin films respectively.

Table 2 The local magnetic moment, m, in Bohr Magnetrons, the Fermi contact hyperfine field, B_{hf} in Teslas, the isomer shift and δ (relative to α-Fe) in mm/s at Fe sites versus different arrangements of 4 Ga atoms in the supercell

		S1	S2	S3	S4
m (μ_B)	A	1.95	2.04	2.08	2.1(A)/2.57(D)
	D	2.45	2.48	2.59	2.42/2.54
B_{hf} (T)	A	25.0	25.0	26.2	24.8(A)/28.3(D)
	D	33.0	29.6	29.3	31.9/31.9
δ (mm/s)	A	0.24	0.20	0.18	0.20(A)/0.04(D)
	D	0.04	0.04	0.04	0.06/0.04

The A and D refer to sites in DO_3 structure (denoted here by S1) and equivalent sites in the other structures

We considered the DO_{22} structure that can be obtained from the DO_3 unit cell by a Bain transformation and tetragonal distortion. We found that with increasing values of the lattice constant*c*, the magnetic hyperfine fields of the A and D sites are roughly maintained, whereas the isomer shift at the site equivalent to D site increases considerably. This increase is attributed to the conversion of four of the Ga atoms from being next nearest neighbors of Fe in bcc structure towards being nearest neighbors in fcc structure. Hence, a sizeable increase in the isomer shift of the D site can be used as an indicator of the presence of DO_{22} phase in alloys. We conclude that the main signature of the presence of the DO_{22} phase is the large increase in the isomer shift of sites that are equivalent to the D site.

4 Conclusion

The contact magnetic hyperfine fields, isomer shifts and local magnetic moments at Fe sites in iron-gallium alloys were calculated versus the number of Ga nearest neighbors. It is found that the contact hyperfine field follows the experimental trends in general. The hyperfine properties were calculated for different phases and different arrangements of atomic positions for the DO_3 phase. Minor changes in the calculated quantities were found. A big change in the isomer shift at Fe D site is found when the DO_3 phase transforms to DO_{22} phase through Bain transformation.

Calculation on larger supercells would allow for studying the effect of more neighbors and the possibility of presence of sizeable cubic and non-cubic clusters of atoms within the large cubic supercell. This may lead to understanding of the role of embedded structures like S2 and of precipitates in the magnetostriction of Fe-Ga alloys.

References

1. Atulasimha, J., Flatau, A.B.: A review of magnetostrictive iron-gallium alloys. Smart Mater. Struct. **20**(4) (2011). doi:10.1088/0964-1726/20/4/043001
2. Xing, Q., Du, Y., McQueeney, R.J., Lograsso, T.A.: Structural investigations of Fe-Ga alloys: Phase relations and magnetostrictive behavior. Acta Mater. **56**(16), 4536–4546 (2008). doi:10.1016/j.actamat.2008.05.011
3. Cullen, J., Zhao, P., Wuttig, M.: Anisotropy of crystalline ferromagnets with defects. J. Appl. Phys. **101**(12) (2007). doi:10.1063/1.2749471

4. Cullen, J.R., Clark, A.E., Wun-Fogle, M., Restorff, J.B., Lograsso, T.A.: Magnetoelasticity of Fe-Ga and Fe-Al alloys. J. Magn. Magn. Mater. **226–230**(PART I), 948–949 (2001)
5. Petculescu, G., Ledet, K.L., Huang, M., Lograsso, T.A., Zhang, Y.N., Wu, R.Q., Wun-Fogle, M., Restorff, J.B., Clark, A.E., Hathaway, K.B.: Magnetostriction, elasticity, and D03 phase stability in Fe-Ga and Fe-Ga-Ge alloys. J. Appl. Phys. **109**(7) (2011). doi:10.1063/1.3535444
6. Du, Y., Huang, M., Chang, S., Schlagel, D.L., Lograsso, T.A., McQueeney, R.J.: Relation between Ga ordering and magnetostriction of Fe-Ga alloys studied by x-ray diffuse scattering. Phys. Rev. B - Condens. Matter Mater. Phys. **81**(5) (2010). doi:10.1103/PhysRevB.81.054432
7. Xing, Q., Lograsso, T.A.: Magnetic domains in magnetostrictive Fe-Ga alloys. Appl. Phys. Lett. **93**(18) (2008). doi:10.1063/1.3013575
8. Golovin, I.S., Dubov, L.Y., Funtikov, Y.V., Palacheva, V.V., Cifre, J., Hamana, D.: Study of ordering and properties in Fe-Ga alloys With 18 and 21 at. pct Ga. Metall. Mater. Trans. A: Phys. Metall. Mater. Sci. **46**(3), 1131–1139 (2015). doi:10.1007/s11661-014-2721-3
9. Cao, H., Bai, F., Li, J., Viehland, D.D., Lograsso, T.A., Gehring, P.M.: Structural studies of decomposition in Fe-x at. %Ga alloys. J. Alloys Compd. **465**(1–2), 244–249 (2008). doi:10.1016/j.jallcom.2007.10.080
10. Quinn, C.J., Grundy, P.J., Mellors, N.J.: The structural and magnetic properties of rapidly solidified Fe 100-xGax alloys, for 12.8=x=27.5. J. Magn. Magn. Mater. **361**, 74–80 (2014). doi:10.1016/j.jmmm.2014.02.004
11. Khachaturyan, A.G., Viehland, D.: Structurally heterogeneous model of extrinsic magnetostriction for Fe-Ga and similar magnetic alloys: Part I. Decomposition and confined displacive transformation. Metall. Mater. Trans. A: Phys. Metall. Mater. Sci. **38 A**(13), 2308–2316 (2007). doi:10.1007/s11661-007-9253-z
12. Cao, H., Gehring, P.M., Devreugd, C.P., Rodriguez-Rivera, J.A., Li, J., Viehland, D.: Role of nanoscale precipitates on the enhanced magnetostriction of heat-treated galfenol (Fe1-xGax) alloys. Phys. Rev. Lett. **102**(12) (2009). doi:10.1103/PhysRevLett.102.127201
13. Laver, M., Mudivarthi, C., Cullen, J.R., Flatau, A.B., Chen, W.C., Watson, S.M., Wuttig, M.: Magnetostriction and magnetic heterogeneities in iron-gallium. Phys. Rev. Lett. **105**(2) (2010). doi:10.1103/PhysRevLett.105.027202
14. Mudivarthi, C., Laver, M., Cullen, J., Flatau, A.B., Wuttig, M.: Origin of magnetostriction in Fe-Ga. J. Appl. Phys. **107**(9), 3 (2010)
15. Du, Y., Huang, M., Lograsso, T.A., McQueeney, R.J.: X-ray diffuse scattering measurements of chemical short-range order and lattice strains in a highly magnetostrictive Fe0.813Ga0.187 alloy in an applied magnetic field. Phys. Rev. B - Condens. Matter Mater. Phys. **85**(21) (2012). doi:10.1103/PhysRevB.85.214437
16. Mellors, N.J., Zhao, X., Simmons, L.M., Quinn, C.J., Kilcoyne, S.H.: A Mössbauer spectroscopy and neutron diffraction study of magnetostrictive, melt-spun Fe-Ga alloy ribbons. J. Magn. Magn. Mater. **324**(22), 3817–3823 (2012). doi:10.1016/j.jmmm.2012.06.021
17. Newkirk, L.R., Tsuei, C.C.: Mössbauer study of hyperfine magnetic interactions in Fe-Ga solid solutions. Phys. Rev. B **4**(11), 4046–4053 (1971). doi:10.1103/PhysRevB.4.4046
18. Dunlap, R.A., McGraw, J.D., Farrell, S.P.: A Mössbauer effect study of structural ordering in rapidly quenched Fe-Ga alloys. J. Magn. Magn. Mater. **305**(2), 315–320 (2006). doi:10.1016/j.jmmm.2006.01.020
19. Basumatary, H., Palit, M., Chelvane, J.A., Pandian, S.: Disorder trapping in gas quenched magnetostrictive Fe-Ga alloys. Mater. Sci. Eng. B: Solid-State Mater. Adv. Technol. **167**(3), 210–213 (2010). doi:10.1016/j.mseb.2010.02.021
20. Bachowski, A., Ruebenbauer, K., Zukrowski, J., Przewoźnik, J.: Charge and spin density on iron nuclei in the BCC Fe-Ga alloys studied by Mössbauer spectroscopy. J. Alloys Compd. **455**(1–2), 47–51 (2008). doi:10.1016/j.jallcom.2007.01.063
21. Bachowski, A., Wdowik, U.D.: Impurity effect on charge and spin density in −Fe - Comparison between cellular model, ab initio calculations and experiment. Acta Phys. Pol. A **119**(1), 24–27 (2011)
22. Wang, H., Zhang, Z.D., Wu, R.Q., Sun, L.Z.: Large-scale first-principles determination of anisotropic mechanical properties of magnetostrictive Fe-Ga alloys. Acta Mater. **61**(8), 2919–2925 (2013). doi:10.1016/j.actamat.2013.01.046
23. Wang, H., Zhang, Y.N., Yang, T., Zhang, Z.D., Sun, L.Z., Wu, R.Q.: Ab initio studies of the effect of nanoclusters on magnetostriction of Fe1-x Gax alloys. Appl. Phys. Lett. **97**(26) (2010). doi:10.1063/1.3533659
24. Boisse, J., Zapolsky, H., Khachaturyan, A.G.: Atomic-scale modeling of nanostructure formation in Fe-Ga alloys with giant magnetostriction: Cascade ordering and decomposition. Acta Mater. **59**(7), 2656–2668 (2011). doi:10.1016/j.actamat.2011.01.002

25. Blaha, P., Schwarz, K., Madsen, G.K.H., Kvasnicka, D., Luitz, J.: In: Schwarz, K. (ed.) WIEN2k: an augmented plane wave + local orbitals program for calculating crystal properties) Technische Universitat Wien, Austria, Vienna (2009)
26. Borrego, J.M., Blázquez, J.S., Conde, C.F., Conde, A., Roth, S.: Structural ordering and magnetic properties of arc-melted FeGa alloys. Intermetallics **15**(2), 193–200 (2007). doi:10.1016/j.intermet.2006.05.007
27. Javed, A., Szumiata, T., Morley, N.A., Gibbs, M.R.J.: An investigation of the effect of structural order on magnetostriction and magnetic behavior of Fe-Ga alloy thin films. Acta Mater. **58**(11), 4003–4011 (2010). doi:10.1016/j.actamat.2010.03.023